

## A COMPUTER MODEL OF MAMMALIAN CEREBELLAR CORTEX

JAMES A. MORTIMER\*

Laboratory of Applied Studies, Division of Computer Research and Technology, National Institutes of Health,  
Bethesda, Maryland, 20014, U.S.A.

(Received 27 October 1972 and in revised form 6 April 1973)

**Abstract**—A computer-simulated model of mammalian cerebellar cortex is described, in which the individual units correspond to 300  $\mu\text{m}$  square regions of the cerebellar cortical sheet. Local properties of these units as well as their pattern of connectivity were derived from anatomical and physiological data. Selection of an appropriate set of parameters produced predicted neuronal firing patterns and excitability changes similar to those obtained from anesthetized cats.

The role of Purkinje recurrent collaterals was investigated by varying the strength of Purkinje cell inhibitory coupling to Golgi and basket cells. It is shown that the recurrent collaterals may exert important effects upon the time course of Purkinje cell responses to parallel fiber inputs. For spatially-distributed mossy fiber inputs, a focusing effect of long time course is demonstrated.

Cerebellum      Cerebellar cortex      Model      Computer simulation      Cellular automata

### INTRODUCTION

The acquisition of detailed information about the microanatomy and electrophysiology of the cerebellar cortex has stimulated much speculation concerning the functional operation of the cerebellar circuit. Several specific hypotheses have been proposed [1-7]. Because of the difficulty of designing experiments that can be performed in the laboratory, however, most of these hypotheses have not received an adequate test.

The construction of the computer simulation model described in the present paper was guided by two major objectives: (1) to provide a working model in which to examine existing views of cerebellar cortical operation; and (2) to suggest new hypotheses that can be tested in the laboratory. Insofar as possible, the parameters of the model were selected to correspond to experimentally-measurable quantities, e.g. the lengths and orientation of different types of intracortical fibers and time courses of post-synaptic potentials. Modification of the model in accord with new anatomical and physiological data is therefore facilitated and a meaningful interaction between simulation and experiment made possible.

PELLIONISZ and SZENTÁGOTHAÏ [8] have recently described a computer model for the cerebellar neuronal network, which allows the evolving spatio-temporal pattern of activity in the cerebellar cortex to be simulated. Its application, however, has thus far been restricted to the study of mutual interactions between only two populations of cerebellar neurons, the Golgi and granule cells. The computer model to be described here differs from their model in two significant ways: (1) all major functional populations of cerebellar cortical neurons are considered; and (2) the primitive units represent aggregates of neurons located within small regions of the cerebellar cortical sheet, rather than single neurons.

\* Present address: Department of Neurosurgery, University of Minnesota Medical School, Minneapolis, Minnesota, U.S.A. and Surgical Service, Veterans Administration Hospital, Minneapolis, Minnesota, U.S.A.

One consequence of selecting larger primitive units is that firing configurations of neurons within a unit region are considered to be identical, if the mean levels of activity in the main populations of cerebellar neurons in this region are the same. In this respect, the present model differs from other recently-proposed cerebellar model [2,4], which attribute functional significance to the detailed spatio-temporal pattern of activity in the cerebellar granule cells. While such a specific functional dependence is not excluded by the assumptions made below, the principal aim of the stimulation is to investigate the relationship between the known structure of the cerebellar network and the more global pattern of neuronal activity resulting from natural and electrical inputs to the cerebellum.

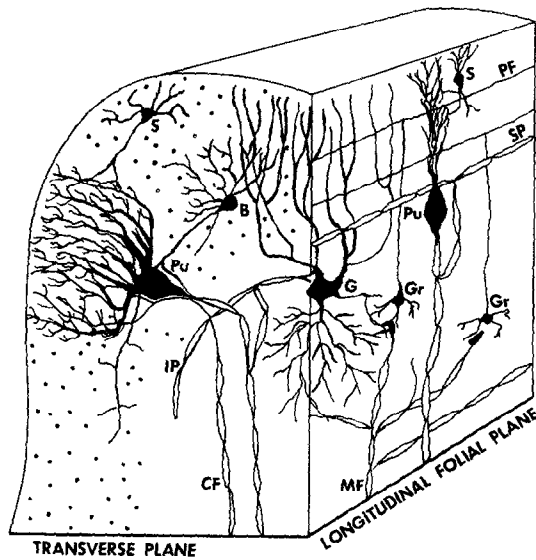


Fig. 1. Schematic drawing of a single folium of cat cerebellar cortex. Description in text.

In this paper two applications of the model will be described. In the first, the role of the Purkinje recurrent collaterals is explored by varying the relative strength of these connections and examining the effects upon simulated Purkinje cell responses to parallel fiber inputs. In the second, the sequence of granule cell activity in the network induced by a spatially-distributed mossy fiber input is studied. Additional questions raised by the simulation results will be considered in a subsequent paper [9].

### *The cerebellar circuit*

Figure 1 summarizes the principal features of the arrangement of neuronal elements in one folium of the cat cerebellar cortex [1, 10]. Two sets of input fibers terminate in the cerebellum. One of these, the mossy fibers (MF), branch extensively and end in excitatory contacts upon dendrites of granule cells in the innermost or granular layer of cortex. Each granule cell (Gr) sends its axon into the outer (molecular) layer, where it bifurcates and runs parallel to the folial axis for a distance of 2–3 mm, contributing to a dense mass of axons called the parallel fibers (PF). Along their course, the parallel fibers make synaptic contact with the dendrites of Purkinje (Pu), Golgi (G), basket (B) and stellate (S) cells, which extend into the molecular layer. The Golgi cells, whose somatae are situated in the granular layer, also receive direct input from the mossy fibers. From each of the Golgi

cells, a dense axonal plexus descends to terminate on the dendrites of granule cells. The axons of basket and stellate cells extend in a plane transverse to the axis of the folium and terminate on the dendrites and pre-axon region of Purkinje cells.

The sole output from the cortex is provided by Purkinje cell axons, which descend through the granular layer, giving off recurrent collaterals that return to the region of the cell body and contribute to plexuses directly above and below the layer of Purkinje cell somata. The upper or supraganglionic plexus (SP)\* is generally considered to be oriented in the same direction as the parallel fibers, while the lower or infraganglionic plexus (IP) is believed to extend in a transverse direction. Physiological [13] as well as anatomical [10, 11, 14, 15] evidence suggests that the axons of these plexuses have as their principal targets the somata of Golgi and basket cells.

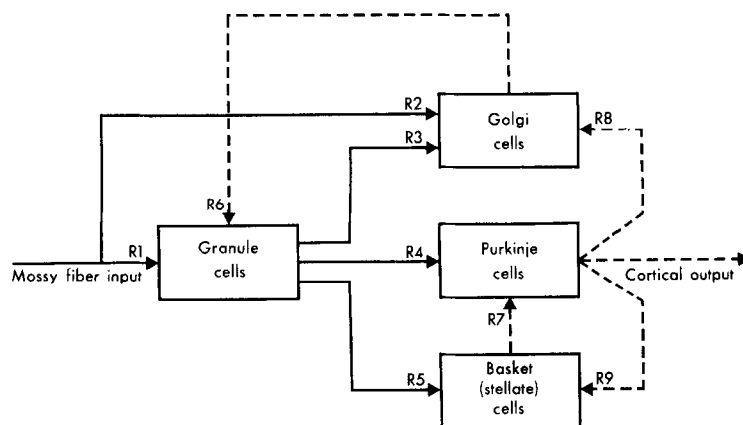


Fig. 2. Block diagram of simplified cerebellar circuit. Excitatory connections are represented by solid lines, inhibitory connections by dashed lines. Strength of connections are determined by coupling coefficients  $R_1$ – $R_9$ .

The extensive physiological investigations of ECCLES *et al.* [1] have shown that with the exception of granule cells, all cerebellar cortical neurons are inhibitory.

In the model, attention will be restricted to the effects of mossy fiber inputs on the pattern of neuronal activity in the cerebellar cortex. The influence of the second set of inputs, the climbing fibers, will not be considered.† A block diagram of the circuit investigated in the simulation is presented in Fig. 2.

### Modeling approach

In the model described below, the cerebellar cortex is represented by a checkerboard array, in which each square corresponds to a  $300 \times 300 \mu\text{m}$  region of the cerebellar cortical sheet. Within each of these regions the neurons may be grouped into five functional populations of active elements: mossy fibers, granule cells, Golgi cells, Purkinje neurons and basket or stellate cells. Output from one of these regions to other regions is conveyed through the axons of neurons whose cell bodies are located in the correspond-

\* The relative importance of this plexus has been questioned by MUGNAINI [11], who claims that most of the myelinated fibers in the lower molecular layer are parallel fibers rather than Purkinje axon collaterals. A projection of Purkinje cell axons onto neurons located in the lower portion of the molecular layer (Purkinje and basket cells), however, has been confirmed in EM studies [12].

† Possible functional roles of climbing fibers have been considered in a number of recent papers [2, 16–20].

ing block of cortex. The state of this output will be considered to reflect the average firing frequency or excitability of each of the five populations of active elements in that region of cortex at a given instant of time. The inputs to a region, on the other hand, are simply those axons terminating in that portion of the cerebellar cortex, and their state will be defined by the outputs from other regions in the checkerboard array as well as by the states of mossy fiber inputs. While this notion of state is sufficient to describe the transmission of information within the cortical sheet, it does not account for the short-term memory that results from temporal summation of synaptic input. To account for this memory the notion of *internal state* will be introduced to represent the cumulative effect of past and present inputs to a region. Finally, from a weighted summation of its cumulative excitatory and inhibitory input (internal state), the output state of a region will be specified.

Connections among various regions in the model are determined by the distinctive spatial patterns of projection of each of the five types of active elements. If the assumption is made that the histology of the cortex is homogeneous, these projections can be represented by a set of templates. When applied to any region the templates will specify those regions from which it receives inputs.

## THE MODEL

It is convenient to consider the two-dimensional array of regions described above as a *cellular automaton system* [21]. A brief description of this representation is given in the appendix to this paper (see also Refs. [22 and 23]). Basically, a cellular automaton system consists of an array of unit regions or *cells*,\* each of which contains an identical finite automaton. Changes in the internal state of these automata occur only at discrete time steps, at which time they also emit an output. The pattern of connection of the finite automata in the array is specified by a template. When applied to any *cell* in the space this template determines which automata provide input to that *cell*.

Since only the average state of activity of the five sets of active elements within each region is considered, each of these five sets may be replaced by a single representative element, hereafter called a *neuron type*. For positive output states, the *output state* of the  $k$ th neuron type in *cell*  $ij$ ,  $O_k^{ij}$ , will be interpreted as the average firing frequency of the  $k$ th set of active elements in the region located at coordinates  $i, j$  in the checkerboard space. Negative output states will represent the amount of additional excitatory input required for the ensemble of neurons represented by the neuron type to reach firing threshold. This quantity provides a measure of the depth of inhibition of a neuronal population within a particular region of the cortical sheet.

Since it is assumed that all information is conveyed through conducted spike activity, the *input state* of a *cell* can be defined in terms of the state of activity of the axons that have synaptic terminations in the region of cortex represented by the *cell*. The state of activity of these axons is a function of the output state of the same or other *cells* in the array. If  $I_m^{ij}$  represents the mean firing frequency of the  $m$ th set of axons terminating in *cell*  $ij$ , then the input state of *cell*  $ij$  can be defined by the vector  $I^{ij} = \langle I_1^{ij}, I_2^{ij}, I_3^{ij}, I_4^{ij}, I_5^{ij}, I_6^{ij} \rangle$ , where the sets of axons are indexed as follows:  $I_1^{ij}$ , mossy fiber;  $I_2^{ij}$ , parallel fiber (granule);  $I_3^{ij}$ , Golgi;  $I_4^{ij}$ , basket (stellate);  $I_5^{ij}$ , Purkinje infraganglionic;  $I_6^{ij}$ , Purkinje supraganglionic.

\* To avoid confusion with the biological unit, *cell* in italics will denote the primitive component of a cellular automaton in the remainder of this paper. The unitalicized form will be used synonymously with neuron.

Since the average frequency of spike discharge never falls below zero, the input state will always be a nonnegative vector. (Negative output states are not transmitted and reflect only the local state of excitability of an ensemble of neurons.)

Each type of neuron receives inputs from a distinct subset of the set of active elements in the cortex. In general, these inputs may have different effects (excitatory or inhibitory) and different time constants of synaptic decay. It will be assumed that at any time the history of activity of a particular set of axons terminating in a cellular region is encoded in the temporal summation of post-synaptic potentials. Therefore, the *internal state* of a cellular region,  $S^{ij}$ , can be defined as a vector of temporally-summed amplitudes of six different synaptic inputs  $\langle S_1^{ij}, S_2^{ij}, S_3^{ij}, S_4^{ij}, S_5^{ij}, S_6^{ij} \rangle$ , corresponding to the six sets of axons described above. This vector will constitute the only memory in the system, since long-term changes in synaptic effect will not be considered.

The set of *cells* from which a particular neuron type receives input will be defined as the *neighborhood* of that neuron type. In the model, the neighborhoods of the neuron types are determined by the distinctive spatial patterns of projection of the five kinds of active elements. Because the probabilities of synaptic connection are likely to vary with the distances between *cells*, it is necessary to provide a means of specifying these probabilities. This is accomplished in the model by associating with each *cell* in the neighborhood a weight corresponding to the relative frequency with which a connection of the indicated type is likely to occur. The selection of the neighborhoods as well as of the associated sets of weights was made on the basis of the following assumptions derived from anatomical observations of the cat cerebellar cortex:

- (i) Parallel fibers were assumed to project to Purkinje, basket, stellate, and Golgi cells located in the same folial plane as the granule cell body. The lengths of parallel fibers were considered to be normally distributed with a mean of 3 mm [1] and a standard deviation of 500  $\mu\text{m}$ .
- (ii) The dendrites and axonal plexus of Golgi cells were assumed to occupy spatial compartments 600  $\mu\text{m}$  in diameter [1].
- (iii) The synaptic terminals of basket and stellate cells were considered to be distributed to an area extending 1 mm transverse to the folial axis and 250  $\mu\text{m}$  along it in both directions [24]. In the absence of specific data, the likelihood of synaptic contact with a Purkinje cell was assumed to decrease exponentially with distance in both the longitudinal (folial) and transverse directions.
- (iv) The Purkinje recurrent collaterals were assumed to project to basket and Golgi cells located close to the Purkinje cell of origin [25]. In the model, this assumption was realized by making the probability of synaptic connection an exponentially-decreasing function of distance and requiring that one-half of the synaptic contacts be made within 0.5 mm of the cell of origin of the fiber. In accord with the general orientation of the plexuses, those recurrent collaterals projecting to basket cells were assumed to run parallel to the folial axis in the supraganglionic plexus and those projecting to Golgi cells to run primarily in a transverse direction in the infraganglionic plexus.

The set of neuron-type neighborhoods resulting from these assumptions is shown in Fig. 3 for the main functional populations of cortical neurons. By applying the templates illustrated in this figure to any *cell* in a two-dimensional array, the spatial pattern of inputs to that *cell* can be determined. The relative strength of any particular connection between

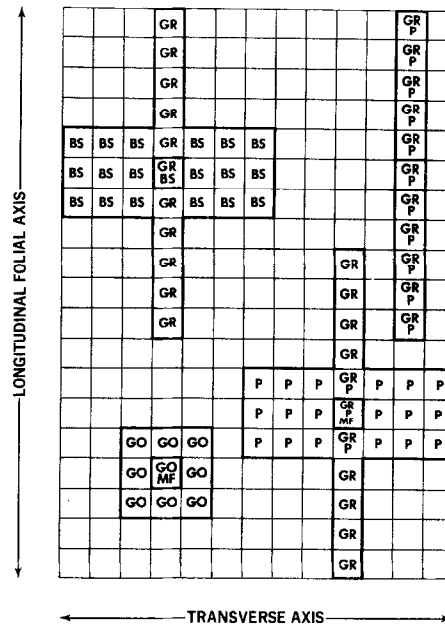


Fig. 3. Connection templates (neighborhoods) for cerebellar cortex model. Letters in squares identify 300  $\mu$ m square cellular regions from which neurons of the indicated type project to the central cell (shown in heavy outline). Upper left: inputs to Purkinje cells, upper right: inputs to basket (stellate) cells, lower left: inputs to granule cells, lower right: inputs to Golgi cells. P: Purkinje, BS: basket (stellate), MF: mossy fibers, GO: Golgi, GR: granule.

two cells depends upon the relative location and distance between these cells as described above.

Since the cortex is assumed to be a uniform sheet, every cell in the model contains an identical finite automaton and it is sufficient to specify a single transition function. This function can be expressed as a set of difference equations:\*

$$S_m^{ij}(t+1) = B_m S_m^{ij}(t) + I_m^{ij}(t), m = 1, \dots, 6 \quad (1)$$

where  $S_m^{ij}(t)$  is the internal state and  $I_m^{ij}(t)$ , the input state, of the  $m$ th set of axons terminating in cell  $ij$  at time  $t$ , and  $B_1, \dots, B_6$  are constants representing the rates of decay of the post-synaptic potentials for the six sets of axons considered.

The output state of each neuron type is obtained from a weighted algebraic summation of the internal states of its inputs. Taking into account the circuitry of the cortex, the output function of the finite automaton can be defined by a set of five equations:

$$\begin{aligned} O_1^{ij}(t) &= I_1^{ij}(t) \\ O_2^{ij}(t) &= R_1 S_1^{ij}(t) - R_6 S_3^{ij}(t) - T_2 \\ O_3^{ij}(t) &= R_2 S_1^{ij}(t) + R_3 S_2^{ij}(t) - R_8 S_5^{ij}(t) - T_3 \\ O_4^{ij}(t) &= R_4 S_2^{ij}(t) - R_7 S_4^{ij}(t) - T_4 \\ O_5^{ij}(t) &= R_5 S_2^{ij}(t) - R_9 S_6^{ij}(t) - T_5 \end{aligned} \quad (2)$$

\* The local transition function of the cellular automaton system (see Appendix) is obtained from these equations by substituting a weighted summation of output states over the neighborhood for each of the  $I_m^{ij}(t)$ . The weights reflect the probabilities of synaptic connection with distance described above.

where  $S_1^{ij}, \dots, S_6^{ij}$  are defined by the transition function;  $I_1^{ij}(t)$  represents the mossy fiber input to cell  $ij$  at time  $t$ ;  $O_1^{ij}(t), \dots, O_5^{ij}(t)$  represent the output states of mossy fibers, granule cells, Golgi cells, Purkinje cells and basket or stellate cells, respectively, and  $R_1, \dots, R_9, T_2, \dots, T_3$  are parameters.

The relative influence of synaptic inputs to particular types of neurons in the cerebellar cortex is represented in the model by the coupling coefficients  $R_1$ – $R_9$  (see Fig. 2). These parameters account for the numbers of synaptic contacts each kind of neuron receives from the other sets of active elements as well as the average strength of individual contacts. Since the values given to  $T_2$ – $T_5$  in the simulation runs to be described are negligible in comparison to the other terms in the set of equations (2), the effect of these parameters on the simulation output will not be considered in this paper.

#### *Selection of synaptic time constants*

The values of the parameters ( $B_1$ – $B_6$ ) in equation (1) were selected, insofar as possible, by fitting published data on the time course of post-synaptic potentials (PSP's). The only post-synaptic potentials that have been recorded intracellularly in the cerebellar cortex are the IPSP resulting from basket cell input to Purkinje cells and the EPSP produced by the action of parallel fibers on the Purkinje cell [1]. These two post-synaptic potentials were fitted by the exponential functions:

$$y_i = e^{-0.058t} \quad (t \text{ in msec})$$

for the inhibitory input, and

$$y_e = e^{-0.066t} \quad (t \text{ in msec})$$

for the excitatory input. Since no data were available on the time courses of other post-synaptic potentials in the cortex, it was assumed that all IPSP's had time constants of decay equivalent to the basket cell IPSP, and that all EPSP's had similar time courses to the parallel fiber-induced EPSP in Purkinje cells.

## COMPUTER SIMULATION

The definitions of neighborhood, transition and output functions given above specify local properties of the cerebellar network. To gain insight into the global behavior of the network resulting from these local properties, a  $20 \times 20$  array of cells, corresponding to a 6 mm square block of cortex, was simulated. In order to avoid boundary discontinuities, two geometries were assumed. In the first, the  $20 \times 20$  array was considered to cover the surface of a torus, so that the neighbors of every cell in the array were also located in the array. This geometry is especially suitable for investigating the stability of the network, since no unwarranted stabilizing effect is introduced by assigning the cells outside of the array an arbitrary fixed state. However, since perturbations introduced in the network can propagate, there is a possibility that this wrap-around geometry may introduce undesirable interactions. Therefore, the toroidal geometry was employed only to establish a stable level of background activity. This level was then used to assign to cells outside of the array a fixed vector of output states to represent the diffuse background activity in surrounding regions of cortex.

Input to the cerebellar cortex was assumed to be of three types: (1) a diffuse background discharge of mossy fibers, (2) a non-random perturbation of mossy fiber input, and (3) local electrical stimuli applied to the cerebellar surface. To simulate (1), the output states of all mossy fiber neuron types in the array were, at each time step, selected randomly from a

distribution whose mean was set as a parameter of the model. This activity then served as the driving force behind all other activity in the network. Inputs (2) and (3) were specified by defining the sets of *cells* in the array receiving the input and a corresponding sequence of input values, which were used to augment the output states of selected neuron types in these *cells* on successive time steps. A local electrical stimulus to the cerebellar surface, for example, was simulated by augmenting the output states of particular granule neuron types for a given number of time steps.

In order to compare the simulation output to physiological data, three methods of output presentation were used:

- (1) "snapshots" of the output states of each neuronal population over the entire network at successive time steps;
- (2) graphs of the output state of a *cell* as a function of time; and
- (3) predictions of typical firing patterns for neurons of a given type in a particular region of the simulated block of cortex.

The latter output was generated in the following way: The activity of an ensemble of neurons was assumed to be governed by the level of a pool of excitation (cumulative output state), which was augmented by excitatory synaptic input and decremented by inhibitory input. When the pool reached a critical level, an impulse was predicted, the pool emptied, and the process repeated to determine the time of occurrence of the next impulse. Because additions to the pool during a time step could be larger than required for a single impulse to occur, the time of occurrence of the impulse or impulses was a function of the size of the additional excitatory input occurring on that time step.

## COMPUTER IMPLEMENTATION

The simulation program was run on an IBM 1800 with 16K of core memory and associated disk storage. A DEC 338 display under the control of a PDP-7 provided at run time a spatial representation of the current state of the model and permitted interaction with the program by means of a light pen. Additional input to the simulation could be entered through the keyboard of the PDP-7, which was connected with the IBM 1800 through a high-speed interface.

A simulation system for cellular automata [26] provided the software nucleus of the simulation program. This system, which consists of a set of assembly language programs written for the IBM 1800 and PDP-7, offered a great deal of flexibility in the initial specification of such parameters as the geometry and connectivity of the network, as well as permitting changes in these and other characteristics at run time. The main simulation routine as well as many of the subroutines were written in FORTRAN.

An extensive command language permitted run time changes in model parameters, definition of inputs in space and time, and specification of variables to be displayed or saved on disk for further analysis. The consecutive states of the network were computed for 3 msec time steps, and a complete record of the simulation output kept on single frames of movie film.

## STABILITY OF THE NETWORK STATE

To assess the validity of the model, agreement was initially sought between the model's predictions and the data collected by ECCLES *et al.* [1, 27-31] on the response of cerebellar



neurons in the anesthetized cat to local electrical stimuli applied to the surface of the cerebellum. Because a systematic search through the parameter space would require a prohibitive amount of computer time, a set of initial runs was carried out to restrict this search to those parameter sets in which the four populations of cortical neurons maintained positive and stable\* output states.

### *Investigation of stability using the computer model*

Through recurrent collaterals Purkinje cells are capable of inhibiting basket neurons which inhibit the same or other Purkinje cells. Furthermore, Purkinje cells can inhibit Golgi neurons, thereby opening the gate to increased parallel fiber excitation, which, in turn, leads to increased activity in Purkinje neurons. These two forms of positive feedback make it possible for Purkinje cells to "take over" the network, by suppressing activity in Golgi, basket, and stellate neurons. Observation of the natural system, however, indicates that this take-over does not occur; indeed, a balance seems to be achieved whereby the four populations of cortical neurons exhibit continuous spontaneous activity [1]. It is, therefore, of interest to determine whether such a steady state can be maintained in the presence of background levels of mossy fiber input. To investigate this question, an initial series of runs was carried out. Since the coupling coefficients cannot be directly determined from physiological or anatomical data, the set of parameters for these runs was chosen on the basis of plausible assumptions regarding the relative importance of particular synaptic connections. The following initial parameter assignments were made:

- (i) The coupling coefficient from mossy fibers to granule cells ( $R_1$ ) was assigned a value twice that of the coefficient from Golgi cells to granule cells ( $R_6$ ).
- (ii) The coupling coefficient of parallel fiber input to Golgi cells ( $R_3$ ) was given a value twice that of the mossy fibre input to these cells ( $R_2$ ) and four times that of the input from the Purkinje infraganglionic plexus ( $R_8$ ).
- (iii) Similarly, the excitatory input from granule neurons to basket and stellate cells ( $R_5$ ) was assumed to be almost seven times as powerful as the inhibitory input from Purkinje neurons to these cells ( $R_9$ ).
- (iv) The coupling coefficient from granule cells to Purkinje cells ( $R_4$ ) was assigned a value three times that of the coupling coefficient from basket (stellate) cells to Purkinje neurons ( $R_7$ ).

Although a stable level of background activity could be maintained in all populations of representative neuronal elements with these parameter values, the simulated on-beam response of Purkinje cells to a strong parallel fiber input included up to four spikes. In order to bring the simulated discharge into agreement with the evoked discharge observed in barbiturate-anesthetized cats [1],  $R_4$  was decreased by a factor of four. After this modification, even very large parallel fiber inputs never produced more than one evoked spike.

With this amended set of parameters, the four populations of representative neuron types maintained stable, non-zero firing rates in the presence of a continuous background level of mossy fiber activity. Exploration of the parameter space revealed that the most important parameters affecting the stability of network activity were the relative strengths of inhibitory and excitatory inputs to each of these four neuronal populations. Whenever the coupling coefficients were adjusted such that the inhibitory inputs to the four populations of cortical neurons were considerably smaller than their excitatory inputs, the

\* For the purposes of this paper, a state will be considered to be stable if, following a small perturbation, the network returns to that state asymptotically.

network exhibited asymptotic stability and returned to the same steady state from a wide range of initial conditions. For the set of coupling coefficients described above it was possible to find a background level of mossy fiber activity, such that the average steady-state firing frequencies predicted for the four neuronal populations (granule: 12/sec, Purkinje: 22/sec, Golgi: 24/sec, basket (stellate): 9/sec) were within the range of observed spontaneous firing frequencies in the anesthetized cat [1]. This set of coefficients and background level of mossy fiber discharge were used in the remainder of simulation runs to be described in this paper and constitute what is referred to subsequently as the *anesthetized model*.

## APPLICATIONS

### *The role of the Purkinje recurrent collaterals*

The functional importance of the Purkinje recurrent collateral system has been questioned by ECCLES *et al.* [1]. In a series of physiological studies of deafferented cerebella [28], only a small inhibitory action was demonstrated on Purkinje cells following antidromic stimulation of their axons. A similar weak inhibition of the Golgi and molecular layer interneurons in intact cerebella was seen after stimulation of the white matter [29]. From these experiments, the inhibitory effectiveness of the recurrent collaterals appeared to be quite limited. Thus, in the theory of cerebellar operation presented by ECCLES *et al.* [1, 32], the Purkinje recurrent collaterals are generally omitted from summary diagrams of the functional circuitry. In a more recent study of deafferented cerebella, LLINÁS and PRECHT [13] showed that a substantial inhibitory action was produced in basket and stellate cells following stimulation of the Purkinje axons. This finding led these investigators to suggest that the predominant function of Purkinje axon collaterals is to regulate the activity of the inhibitory interneurons in the cortex.

In order to examine the influence of the Purkinje axon collaterals, the coupling coefficients from Purkinje to Golgi and basket (stellate) neuron types were systematically varied. Using the anesthetized model, a brief electrical stimulus to the cerebellar surface was simulated by augmenting the output state of the parallel fibers (granule neuron types) in a 300  $\mu\text{m}$  wide "beam" for a single 3 msec time step.\* The simulated time course of Purkinje excitability (output state) at four locations relative to this beam is shown in Figs. 4(A–D). For comparison, an intracellular record from a Purkinje cell following similar stimulation is presented in Fig. 4(E).

Figure 5 shows the predicted spike discharge patterns for on-beam Purkinje, Golgi and basket (stellate) cells following a simulated electrical stimulus to the cerebellar surface, as well as the predicted discharge of a Purkinje cell, 300 and 600  $\mu\text{m}$  off-beam. These simulated discharge patterns illustrate the strong action of a parallel fiber volley on the activity of basket and Golgi cells, and the prolonged inhibition of Purkinje cell discharge resulting from such a volley. The transient on-beam facilitation of Purkinje cells resulting from direct parallel fiber input (Fig. 4A) corresponds to the production of a single spike (Fig. 5A). Following this facilitation a prolonged period of inhibition of on-beam Purkinje activity

\* A brief electrical stimulus to the cerebellar surface is generally considered to affect primarily the parallel fibers situated under the stimulating electrode [1]. Since the parallel fibers extend for approx 3 mm, a local electrical stimulus will excite a narrow "beam" of parallel fibers about 6 mm in length. References to the distance off-beam refer to the distance measured in a transverse direction from the center of an activated beam of parallel fibers.

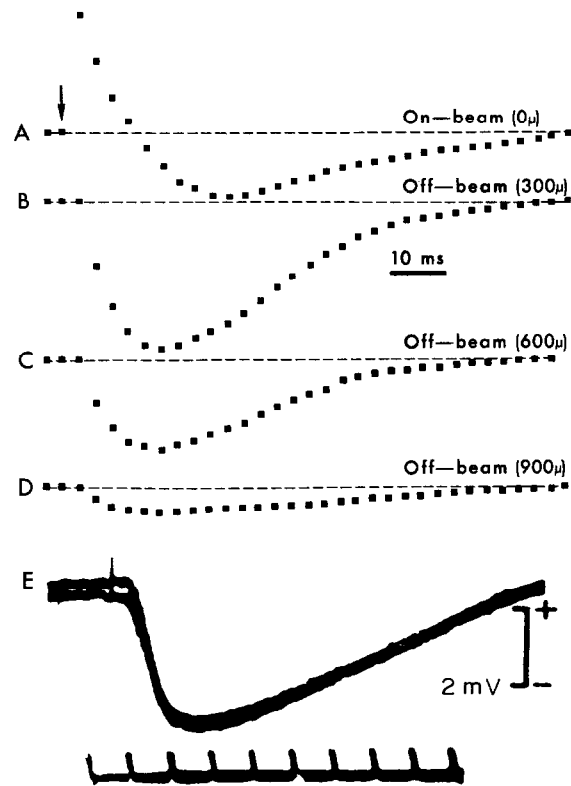


Fig. 4. Response of Purkinje cells to local electrical stimulation of the cerebellar cortical surface. (A-D). Simulated response (output state) of Purkinje cells on-beam, and 300, 600 and 900  $\mu$ m off-beam. Onset of simulated 3 msec stimulus shown by arrow in A. (E). Intracellular record from Purkinje cell during application of local electrical stimulus (reproduced from ECCLES *et al.* [1]). Time scale for (E) marked in 10 msec increments.

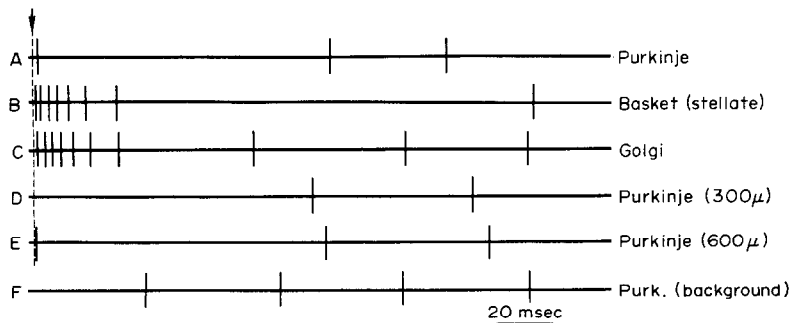


Fig. 5. Predicted discharge patterns of Purkinje, Golgi and basket (stellate) cells following a simulated electrical stimulus to the cerebellar surface (arrow). (A-C) on-beam activity; (D, E) Responses of off-beam Purkinje cells; (F) background Purkinje discharge.

is predicted as a result of the direct inhibitory influence of stellate cells as well as the disfacilitation of Purkinje cells due to the Golgi inhibition of the background granule cell discharge. Since the excitatory influence of parallel fibers is only exerted on-beam, the off-beam influence of the stimulus is restricted to a depression of the output state of Purkinje neurons mediated by the inhibitory action of on-beam basket neurons (Figs. 4B–D, Figs. 5B, D, E).

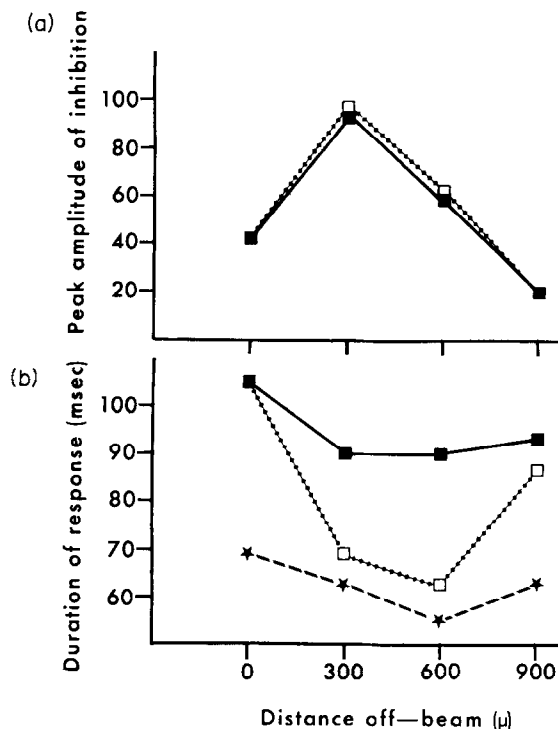


Fig. 6. Effect of Purkinje recurrent collaterals on the maximum negative Purkinje output state following a simulated electrical stimulus (a), and on the duration of the Purkinje response from stimulus onset until return to the background discharge rate (b) at four locations relative to the excited beam of parallel fibers. Filled squares: anesthetized model with both recurrent collateral connections; open squares: same model with all recurrent collateral connections eliminated; stars: model without projection from Purkinje cells to basket and stellate cells. Removal of Purkinje input to Golgi cells is not shown because of no effect in (a) and indeterminate duration of response in (b).

In order to examine the influence of the Purkinje recurrent collaterals on the spatio-temporal pattern of activity produced by a simulated electrical stimulus, three parameters were selected to characterize the response of Purkinje neuron types: (1) time to peak negativity of the output state following the stimulus; (2) maximum negative value of the output state; and (3) duration of the simulated neuronal response from stimulus onset until return of the Purkinje output state to its background level.

Figure 6 summarizes the findings with respect to three cases: (1) absence of recurrent collaterals to basket (stellate) cells ( $R_9 = 0$ ); (2) absence of recurrent collaterals to Golgi cells ( $R_8 = 0$ ); and (3) total elimination of the recurrent collateral connections ( $R_8 = 0$ ,  $R_9 = 0$ ). From (a), in which the maximum amplitude of inhibition (maximum negative output state) is plotted against the distance from the center of the activated beam of parallel

fibers, it is apparent that this parameter of the response is affected only very slightly by the presence or absence of the recurrent collaterals. Similarly, although it is not shown, the time to peak negativity is virtually identical in all three cases. From (b), however, it is apparent that the duration of the neuronal response is quite sensitive to the presence of the collaterals. Although the duration of the on-beam response is the same with recurrent collaterals as without them, the duration of the off-beam inhibition of

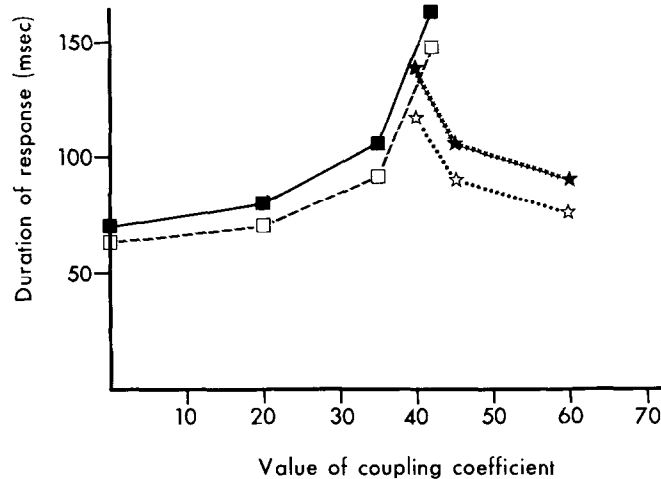


Fig. 7. Effect of strengths of Purkinje axon collateral coupling coefficients on the duration of the Purkinje response on-beam (filled symbols) and 300  $\mu\text{m}$  off-beam (open symbols). Dependence of response duration on coupling coefficient between Purkinje and Golgi cells ( $R_8$ , stars) is compared with dependence on the coupling strength between Purkinje and basket (stellate) cells ( $R_9$ , squares). Anesthetized model:  $R_8 = 45$ ,  $R_9 = 35$ .

Purkinje activity is reduced and shows more variation when the collaterals are eliminated from the circuit. Removal of the collaterals to basket cells only ( $R_9 = 0$ , stars in (b)) produce a uniform reduction in duration at all locations relative to the beam of excited parallel fibers. On the other hand, setting the coupling coefficient from Purkinje to Golgi cells ( $R_8$ ) equal to zero leads to an unstable situation in which the Purkinje neuron types never return to the same spontaneous background firing rate. In the latter case, a new steady state is eventually reached, which gradually spreads and encompasses the entire network.

To understand the significance of these findings, a more detailed investigation was carried out in which  $R_8$  and  $R_9$  were allowed to take on intermediate values. Figure 7 shows the relationship between the value of each of these parameters and the duration of the on-beam and off-beam Purkinje responses to a simulated local electrical stimulus. In each case, the other coupling coefficients are held constant while the relevant parameter is varied. From this figure it is apparent that the duration of the response of Purkinje cells is relatively insensitive to  $R_9$  (squares) for values of this parameter between 0 and 35, but increases very rapidly beyond 35. The dependence of duration on  $R_8$  (stars) exhibits the opposite sensitivity. Increasing  $R_8$  beyond 45 has little effect, but a small decrease in  $R_8$  below 35 leads to a large increase in the duration of depressed Purkinje activity following the simulated stimulus. It is likely that under most physiological conditions these parameters would fall in the flat portions of the curves. However, the great sensitivity of the

duration of the Purkinje cell response to these parameters within certain ranges may provide an explanation for the prolonged periods of inhibition of Purkinje cells following electrical stimulation of the cerebellar cortex which have been observed in some physiological experiments [33].

It is interesting to note that elimination of both plexuses leads to moderate durations of reduced Purkinje activity, despite the fact that elimination of the Purkinje input to Golgi cells alone ( $R_8 = 0$ ) produces an unstable situation, in which the output states of Purkinje cells never return to prestimulus levels. The instability of the network state produced by low values of  $R_8$  must therefore result from an interaction of the inhibitory actions of Purkinje cells on Golgi and basket (stellate) neurons. A possible explanation for this interactive effect is the following:

Inhibition of off-beam Purkinje cells resulting from a local electrical stimulus to the cerebellar surface would lead to disinhibition of off-beam basket and stellate cells through the supraganglionic plexus. The increased firing rates of these basket and stellate cells would then produce a subsequent increase in the inhibition of on-beam Purkinje cells. Since on-beam Purkinje cells are assumed to exert an inhibitory action upon basket and stellate cells in the same folial plane, the discharge rate of on-beam basket cells would be increased through disinhibition, resulting in an even greater inhibition of off-beam Purkinje cells. This regenerative effect would normally be cut short by Golgi inhibition of granule cell activity, bringing about a termination of the evoked basket cell discharge and subsequent recovery of the Purkinje neurons from basket (stellate) inhibition. However, since the only Golgi cells excited by local electrical stimulation of the cerebellar surface would be those situated on-beam, the disfacilitation of basket cells would be restricted to on-beam neurons. If off-beam basket cells became sufficiently disinhibited by the removal of tonic Purkinje inhibition, these cells could serve as a source of instability, that could spread to other portions of the network. Thus, the reciprocal inhibitory connections between Purkinje and basket cells generate a potentially unstable state in the network.

The recovery of activity in the anesthetized model to the same stable firing rates following a stimulated electrical stimulus to the cerebellar surface is apparently due to the inclusion of a moderate Purkinje inhibition of Golgi cells. The suppression of on-beam Purkinje activity by stellate cells following a local electrical stimulus would produce through the infraganglionic plexus a disinhibition of both on- or off-beam Golgi cells. This would cause the firing rates of these disinhibited Golgi cells to increase, thereby reducing the granule cell to off-beam as well as to on-beam basket and stellate cells. In this way, the regenerative increase in basket activity described above would be curtailed. When the Purkinje recurrent collaterals to Golgi cells are eliminated from the circuit, this damping is removed and the steady-state in the network disrupted. Thus, the transverse synaptic connection from Purkinje to Golgi cells provides a spatial damping, which tends to counteract the instability produced by the Purkinje-basket interaction.

An additional effect of the Purkinje projection to Golgi cells may be to partially synchronize the activity of Purkinje cells located in the same sagittal (transverse to folial axis) plane. Inhibition (excitation) of on-beam Purkinje cells would lead to disinhibition (inhibition) of on- and off-beam Golgi cells, thereby tending to equalize the granule cell input to on- and off-beam Purkinje cells. This effect can be seen in Fig. 6(b), where the inclusion of the recurrent collaterals to Golgi cells leads to a more equal duration of on- and off-beam inhibition of Purkinje activity following a simulated local stimulus. The partial synchronization of Purkinje discharge brought about through the recurrent collaterals to

Golgi cells may have functional significance, since restricted regions of the cerebellar nuclei have been shown to receive input from Purkinje cells located in sagittally-oriented strips of cortex [34,35].

#### *Focusing of mossy fiber input*

ECCLES *et al.* [1] suggest that in the case of a spatially-distributed mossy fiber input with a strong central focus of excitation, the action of the weaker peripheral input will be suppressed, while the stronger excitatory input will lead to a beam of active parallel fibers. The overall action will therefore be to transform the input in such a way as to emphasize the strong central portion of a field of active mossy fibers in contrast to its weak surrounds.

Eccles and his coworkers propose that the Golgi cell is the source of this focusing action. Golgi cells, with dendritic trees twice as wide as those of Purkinje neurons, are hypothesized to be strongly excited only in the case of a broad beam of active parallel fibers. Since activation of a Golgi neuron leads to inhibition of granule cells in the region to which it projects, the influence of a diffuse mossy fiber input affecting a broad region of cortex will be suppressed, and the system will favor intense, sharply-localized mossy fiber inputs.

Figure 8 presents the view of Eccles and his colleagues of the hypothetical spatial pattern of granule activity what would emerge during a repetitive mossy fiber input localized to a small region of cortex. The central portion of this diagram (shown in white) represents the zone of intense mossy fiber activation, in which the granule cells are assumed to fire repetitively. Above and below this zone, illustrated by the dark shading, the activity of granule neurons is significantly reduced due to activation of on-beam Golgi cells. Because of the statistical distribution of fiber terminations, these effects are assumed to be reduced on the edges of the excited and inhibited regions, leading to intermediate levels of granule activity shown by the lighter shading.

In order to examine this phenomenon with the computer model, a strong localized mossy fiber input was assumed to be embedded in a region of moderate mossy fiber activity. The spatial pattern of the simulated input is illustrated in Fig. 9 (upper left). To simulate a repetitive discharge of mossy fibers, it was assumed that this input persisted at a constant intensity for a period of 34 time steps (102 msec), after which it returned to the background rate.

The predicted spatial pattern of granule activity at three selected time steps after the onset of the mossy fiber input is shown in Fig. 9. As in the previous figure, the areas of high activity are represented by the lighter shading. From this sequence of "snapshots" of the state of granule cells in the network, it is apparent that this input leads to the gradual suppression of granule activity in most of the regions activated by the moderate mossy fiber discharge, with the resultant focus of active granule cells congruent with the intense mossy fiber input. It is interesting to observe that the formation of this focus was not completed until 19 time steps (57 msec) following the initiation of the simulated mossy fiber input. After this time no additional change in the state of the network was observed, a new steady-state apparently having been achieved. An interesting feature of this steady-state is the ring of active granule cells surrounding the central zone of excitation but separated from it by a trough of inhibition. It is likely that these granule neuron types are active because the Golgi neuron types which would normally inhibit them lack sufficient excitatory input to remain in an active state.

Although the outer ring of active granule neurons is an unexpected finding, the computer simulation output is in substantial agreement with the hypothesis of Eccles and his

### Granule cell excitation

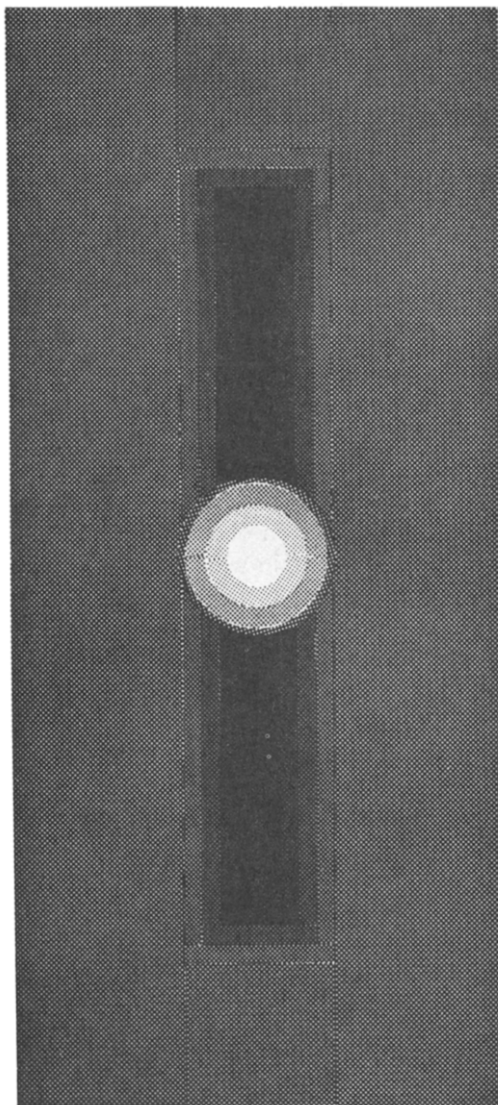


Fig. 8. Postulated spatial pattern of granule activity resulting from a repetitive input localized to a small bundle of mossy fibers. Further description in text. Reproduced from ECCLES *et al.*[1].

colleagues concerning the effects of a repetitive, spatially-distributed mossy fiber discharge. The establishment of a new steady-state after 19 time steps suggests that, once formed, a focus will be maintained by the same input indefinitely. Following an initial transient, therefore, Purkinje, basket and stellate cells, situated on a beam of parallel fibers driven by an intense mossy fiber input, will receive a constant source of excitatory input, while the input to those situated off this beam will be reduced. Although in the normal operation of the cerebellum such idealized inputs probably do not occur, a focusing action must be



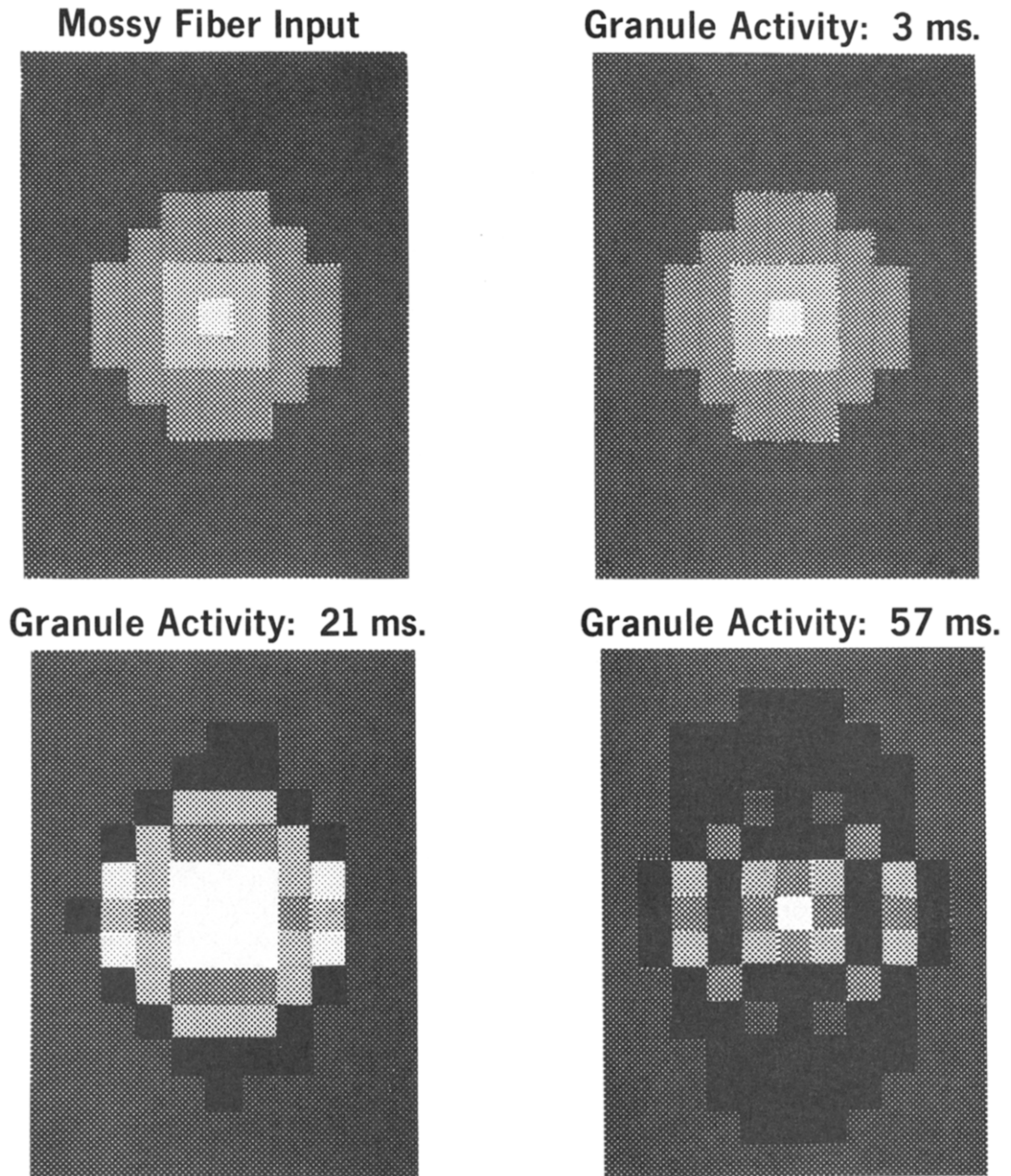


Fig. 9. Simulated pattern of granule activity at three time intervals following the onset of a repetitive mossy fiber input with a strong central focus of excitation. Spatial distribution of simulated input shown in upper left. Areas of high activity are represented by lighter shading; black indicates no activity.

considered as a consequence of the spatial arrangement of elements in the cortex. It is likely that more realistic inputs to the cerebellar cortex will result in a more diffuse spatio-temporal pattern of granule activity than that considered in this example, so that the focusing action, although present, may be less evident.

## CONCLUSIONS

The examples given in this paper were selected to illustrate the consequences of specific connections in the cerebellar circuit as well as of the spatial arrangement of elements in the cortex. From these two examples some tentative conclusions can be drawn.

First, the recurrent collaterals of Purkinje cells probably exert a variety of effects, which should be taken into account in any theory of cerebellar operation. As shown by the simulation, these elements had a substantial effect upon the time course of the Purkinje response to parallel fiber inputs, even though the coupling coefficients assigned to these connections were much smaller than those of other synaptic connections in the model. Thus, demonstration that the connections from Purkinje cells to Golgi and basket cells are quantitatively rare in comparison to other connections in the cerebellar cortex does not exclude the possibility that these elements may play an important functional role in the operation of the mammalian cerebellum. It is also of some interest that the synaptic connections from Purkinje to Golgi cells and those from Purkinje to basket cells may have opposite effects upon the stability of network activity. In this regard, a transverse orientation of the infra-ganglionic plexus seems to be important in maintaining the steady-state of the network in the presence of local perturbations in the state of granule activity. This plexus may also tend to increase the correlation in the spike activity of Purkinje cells that project to cells located in the same regions of the cerebellar nuclei.

Second, given a model in which the simulated response to a local electrical stimulus is similar to that recorded from the anesthetized cat, a prolonged mossy fiber input distributed to a broad region will tend to produce foci of granule activity congruent with the stronger zones of mossy fiber input, while suppressing the granule activity in areas receiving the weaker input. The heightened contrast that would be produced by this action may aid in filtering out noise by emphasizing those regions of the cortical input where much convergence is taking place, while suppressing granule activity in the regions where there is less convergence.

It should be realized, of course, that the eventual effect of the focused granule activity upon Purkinje cells will depend upon the balance attained between stellate and basket cell inhibition and parallel fiber excitation of these cells. The possible role of barbiturate anesthesia in influencing this balance, and therefore the resultant time course of Purkinje cell activity in response to mossy fiber inputs, will be considered in a subsequent paper [9].

## SUMMARY

A computer-simulated model of mammalian cerebellar cortex is described, in which the individual units correspond to 300  $\mu\text{m}$  square regions of the cerebellar cortical sheet. Local properties of the cerebellar network (time course of post-synaptic potentials, patterns of axonal termination, etc.) are derived from anatomical and physiological data. Simulation of a cellular automaton system with these properties permits the spatio-temporal pattern of neuronal activity with a 6 mm square region of the cerebellar cortex to be investigated.

Despite circuit connections in the cerebellar cortex which could lead to unstable network activity, a set of coupling coefficients was found, such that the four populations of cerebellar neurons maintained stable firing rates in the presence of a continuous background level of mossy fiber activity.

The relative strengths of Purkinje inhibition of basket, stellate, and Golgi cells were found to have substantial effects upon the time course of Purkinje responses to parallel fiber inputs. Instability caused by inhibition of basket and stellate cells through the supraganglionic plexus is counteracted by inhibition of Golgi cells through the infraganglionic plexus. The infraganglionic plexus may also serve to increase the correlation in spike activity of Purkinje cells that project to the same regions of the cerebellar nuclei.

In agreement with the speculations of Eccles and his coworkers, prolonged mossy fiber inputs distributed to broad regions of the cerebellar cortex were found to produce foci of granule activity congruent with the stronger zones of mossy fiber input, while suppressing granule activity in areas receiving weaker input.

*Acknowledgements*—This research was initiated in the Department of Computer and Communication Sciences, University of Michigan, Ann Arbor. I would like to thank Profs. H. H. SWAIN, K. C. CASEY, L. K. FLANIGAN and G. C. QUARTON for their advice and suggestions at various stages of this work. I am also grateful to Prof. M. A. ARBIB for his helpful comments on the manuscript.

## REFERENCES

1. J. C. ECCLES, M. ITO and J. SZENTÁGOTHAÍ, *The Cerebellum as a Neuronal Machine*. Springer, New York (1967).
2. D. MARR, A theory of cerebellar cortex, *J. Physiol., Lond.* **202**, 437–470 (1969).
3. J. A. FREEMAN and C. N. NICHOLSON, Space-time transformation in the frog cerebellum through an intrinsic tapped delay-line. *Nature* **226**, 640–642 (1970).
4. J. S. ALBUS, A theory of cerebellar function, *Math. Biosci.* **10**, 25–61 (1971).
5. T. W. CALVERT and F. MENO, Neural systems modeling applied to the cerebellum. *IEEE Trans. Sys. Man Cybernetics* **SMC-2**, 363–374 (1972).
6. S. GROSSBERG, Neural expectation: cerebellar and retinal analogs of cells fired by learnable or unlearned pattern classes, *Kybernetik* **10**, 49–57 (1972).
7. C. C. BOYLLS, The function of the cerebellum and its related nuclei as embedded in a general paradigm for motor control. Ph.D. Thesis, Stanford University (1973).
8. A. PELLIONISZ and J. SZENTÁGOTHAÍ, Dynamic single unit simulation of a realistic cerebellar network model, *Brain Res.* **49**, 83–99 (1973).
9. J. A. MORTIMER, Possible influences of barbiturate anesthesia on cerebellar operation: a computer simulation study. *Int. J. Neurosci.* In press.
10. C. A. FOX, D. E. HILLMAN, K. A. SIEGESMUND and C. R. DUTTA, The primate cerebellar cortex. A Golgi and electron microscope study, *The Cerebellum. Progress in Brain Research*, C. A. FOX and R. S. SINDER (Eds.), Vol. 25, pp. 174–225. Elsevier, Amsterdam (1967).
11. E. MUGNAINI, Ultrastructural studies on the cerebellar histogenesis.—II. Maturation of nerve cell populations and establishment of synaptic connections in the cerebellar cortex of the chick, *Neurobiology of Cerebellar Evolution and Development*, R. LLINÁS (Ed.), pp. 749–782. American Medical Association, Chicago (1969).
12. N. LEMKEY-JOHNSON and L. M. H. LARRAMENDI, Types and distribution of synapses upon basket and stellate cells of the cat cerebellum. An electron microscope study, *J. Comp. Neurol.* **134**, 73–112 (1968).
13. R. LLINÁS and W. PRECHT, Recurrent facilitation by disinhibition in Purkinje cells of the cat cerebellum. *Neurobiology of Cerebellar Evolution and Development*, R. LLINÁS (Ed.), pp. 619–628. American Medical Association, Chicago (1969).
14. J. HÁMORI and J. SZENTÁGOTHAÍ, Identification of synapses formed in the cerebellar cortex by Purkinje axon collaterals: An electron microscope study, *Expl. Brain Res.* **5**, 118–128 (1968).
15. J. HÁMORI and J. SZENTÁGOTHAÍ, Participation of Golgi neurone processes in the cerebellar glomeruli: An electron microscope study, *Expl. Brain Res.* **2**, 35–48 (1966).
16. J. R. BLOEDEL and W. J. ROBERTS, Action of climbing fibers in cerebellar cortex of the cat, *J. Neurophysiol.* **34**, 17–31 (1971).
17. R. LLINÁS, Neuronal operations in cerebellar transactions. *The Neurosciences: Second Study Program*, F. O. SCHMITT (Ed.), pp. 406–426. Rockefeller University Press, New York (1970).
18. R. LLINÁS, J. BLOEDEL and D. E. HILLMAN, Functional characterization of neuronal circuitry in frog cerebellar cortex. *J. Neurophysiol.* **32**, 847–870 (1969).
19. J. T. MURPHY and N. H. SABAHI, Cerebellar Purkinje cell responses to afferent inputs—I. Climbing fiber activation, *Brain Res.* **25**, 449–467 (1971).

20. O. OSCARSSON, The sagittal organization of the cerebellar anterior lobe as revealed by the projection patterns of the climbing fiber system, *Neurobiology of Cerebellar Evolution and Development*, R. LLINÁS (Ed.), pp. 525–537. American Medical Association, Chicago (1969).
21. J. VON NEUMANN, *Theory of Self-reproducing Automata*. University of Illinois Press, Urbana (1966).
22. A. W. BURKS, *Essays on Cellular Automata*. University of Illinois Press, Urbana (1970).
23. E. GOODMAN, R. WEINBERG and R. LAING, A cell space embedding of simulated living cells, *Int. J. Biomed. Computing* **2**, 121–136 (1971).
24. J. SZENTÁGOTHAÏ, The use of degeneration methods in the investigation of short neuronal connexions, *Degeneration Patterns in the Nervous System, Progress in Brain Research*, M. SINGER and J. P. SCHADÉ (Eds.), Vol. 14, pp. 1–32. Elsevier, Amsterdam (1965).
25. C. C. BELL and R. S. DOW, Cerebellar circuitry, *Neurosciences Research Symposium Summaries*, F. O. SCHMITT, T. MELNUCHUK, G. C. QUARTON and G. ADELMAN (Eds.), Vol. 2, pp. 515–616. M.I.T. Press, Cambridge (1967).
26. R. F. BRINDER, A programming system for the simulation of cellular spaces. Ph.D. Thesis. University of Michigan (1970).
27. J. C. ECCLES, R. LLINÁS and K. SASAKI, Intracellularly recorded responses of the cerebellar Purkinje cells, *Expl. Brain Res.* **1**, 161–183 (1966).
28. J. C. ECCLES, R. LLINÁS and K. SASAKI, The action of antidromic impulses on the cerebellar Purkinje cells, *J. Physiol., Lond.* **182**, 316–345 (1966).
29. J. C. ECCLES, R. LLINÁS and K. SASAKI, The inhibitory interneurons within the cerebellar cortex, *Expl. Brain Res.* **1**, 1–16 (1966).
30. J. C. ECCLES, R. LLINÁS and K. SASAKI, The mossy fiber-granule cell relay in the cerebellum and its inhibition by Golgi cells, *Expl. Brain Res.* **1**, 82–101 (1966).
31. J. C. ECCLES, R. LLINÁS and K. SASAKI, Parallel fiber stimulation and the responses induced thereby in the Purkinje cells of the cerebellum, *Expl. Brain Res.* **1**, 17–39 (1966).
32. J. C. ECCLES, The dynamic loop hypothesis of movement control, *Information Processing in the Nervous System*, K. N. LEIBOVIC (Ed.), pp. 245–269. Springer, New York (1969).
33. J. C. ECCLES, D. S. FABER and H. TÁBORIKOVÁ, The action of a parallel fiber volley on the antidromic invasion of Purkyne cells of cat cerebellum, *Brain Res.* **25**, 335–356 (1971).
34. M. ITO and N. KAWAI, IPSP-receptive field in the cerebellum for Deiters neurones, *Proc. Jap. Acad.* **40**, 762–764 (1964).
35. J. JANSEN and A. BRODAL, *Aspects of Cerebellar Anatomy*. Johan Grundt Tanum, Oslo (1954).

## APPENDIX

A *cellular automaton* can be viewed as an infinite checkerboard, in which each square or *cell* contains a copy of the same finite automaton. Each of these automata is able to communicate with a particular subset of the other automata, determined by the topology or connection structure of the two-dimensional space. The connection structure is conveniently formulated in terms of the *neighborhood*, a cell's *neighbors* being those *cells* from which it may receive an input.

At some time,  $t_0$ , each of the finite automata in the checkerboard space is assigned an initial state. Thereafter, the automata assume subsequent states at discrete time steps, which may be represented by unit time intervals ( $t_0, t_0 + 1, \dots$ ). The state transition from one time step to the next is determined uniquely for each finite automaton by a *local transition function*, which takes as arguments the states of the *cell* and its neighbors.

Given a state configuration (an assignment of states to each of the automata), the *global transition function*, defined by the simultaneous application of the local transition function to every *cell* in the space, determines a new state configuration one time step later. The sequence of state configurations generated by the repeated application of this function constitutes a trajectory through the system state space and is generally interpreted as representing the behavior of the system.

A *finite automaton* is a system  $A = \langle I, O, S, \tau, \lambda \rangle$  whose operation is determined as follows:

At each time step  $A$  is in one of a finite set of *internal states*  $S$ . It receives an input from the set of *input states*,  $I$ , and emits an output from the set  $O$ . At the same time it undergoes a change in internal state determined by the *transition function*,  $\tau$ , which gives the next internal state as a function of the present internal state and the current input. If  $I(t)$  represents the input vector and  $S(t)$ , the internal state at time  $t$ , then

$$S(t+1) = \tau(I(t), S(t)). \quad (\text{A.1})$$

The output state that is transmitted is determined by an *output function*,  $\lambda$ , which gives the output at time  $t$  as a function of the internal state at  $t$ . This relationship may be represented by:

$$O(t) = \lambda(S(t)). \quad (\text{A.2})$$

Considering a two-dimensional array of finite automata with a given neighborhood property, the input to any particular automaton is the output from the set of automata in the space defined by the neighborhood. The global transition function of the *cellular automaton system* defined by this array of finite automata can be obtained directly from the transition and output functions of the finite automata together with the neighborhood definition.